

NRL Report 6009

UNCLASSIFIED

Exploding Conductors

Final Report, June 30, 1960 to June 30, 1963

W. R. FAUST, G. E. LEAVITT, J. D. SHIPMAN, JR., AND I. M. VITKOVITSKY

*Analysis and Theory Branch
Radiation Division*

and

F. D. HARRINGTON

*Radiometry Branch
Optics Division*

October 31, 1963



U. S. NAVAL RESEARCH LABORATORY
Washington, D.C.

CONTENTS

Abstract	1
Problem Status	1
Authorization	1
INTRODUCTION	1
ENERGY STORAGE SYSTEMS	2
INSTRUMENTATION DEVELOPMENT	4
EXPERIMENTAL PROCEDURE, DIAGNOSTICS, - AND RESULTS	8
CONCLUDING REMARKS.....	13
REFERENCES	14
APPENDIX A – Time-Resolved Spectroscopy in the Visible Region.....	15

Copies available from Office of Technical Services
Department of Commerce – \$.75

UNCLASSIFIED

Exploding Conductors

Final Report, June 30, 1960 to June 30, 1963

W. R. FAUST, G. E. LEAVITT, J. D. SHIPMAN, JR., AND I. M. VITKOVITSKY

*Analysis and Theory Branch
Radiation Division*

and

F. D. HARRINGTON

*Radiometry Branch
Optics Division*

This report is the summary of the work done at the U.S. Naval Research Laboratory between June 30, 1960 and June 30, 1963. It contains the material that has been discussed in detail in a series of progress reports. In addition, some of the work has been published and is referenced at the end of the report.

The work reported here deals with the investigation of electrically exploded wires in vacuum. The electrical pulses needed for this purpose were provided by the very low inductance capacitors, the development of which was part of the work covered here. The main problems considered were (a) the x-ray, visible, and near ultraviolet emissions from the explosions, (b) the development of the instrumentation needed to determine the time history of the current through and the voltage across the exploding wires, and (c) the relation of the current and voltage to the energy dissipated in the explosion. The techniques that were employed in the study of the various emissions are outlined. The appendix contains detailed discussion of the radiation measurements in the visible range and its analysis.

INTRODUCTION

The work reported here is the continuation of the investigation of the exploding wire phenomena at the U.S. Naval Research Laboratory reported earlier in Ref. 1. It is the purpose of this report to provide a summary of the work performed from June 30, 1960 to June 30, 1963. The details of equipment, experiments and results have been given in a series of progress reports (letter reports) listed collectively as Ref. 2. One aspect of the work covered here, the initial experiments with the production of x-rays in the exploding wires during the electrical discharge, has been described in Ref. 3.

The problem that has been investigated is the emission of x-rays from metallic conductors which are exploded by very high current surges. This phenomena is typical of those discharges in which very high voltages appear across the conductor. This fact necessitated further work on the development of the electrical storage systems characterized by their extremely low inductance and high

voltage operation. One major problem appeared in connection with these storage systems, namely, the measurement of voltage applied across the exploding conductor and the determination of power input producing such explosions. This problem has been solved for some restricted applications; however, it is still plaguing the experiments where it is not possible to confine the discharge current to the exploding conductor. (Some approaches to produce such confinement of current will be discussed more thoroughly in conjunction with the description of an explosion chamber specifically designed to alleviate this problem.)

In addition to the study of x-ray emission, radiation in the visible range has been studied using spectrographs that provide both time-integrated and time-resolved spectra of the emission from exploding conductors. Both continuous and line radiation has been studied and the results will be summarized.

In the field of electrical energy storage, some minor improvements have been made on water-Mylar and water-dielectric capacitors (described in Ref. 1), but the main effort has been directed

NRL Problem H03-21; Project DASA MIPR - 522-61. This is the final report on the problem; the problem has been closed. Manuscript submitted August 27, 1963.

toward achieving the ability to store large amounts of electrical energy at about a level of 10^6 volts. Partial success was achieved by using a specially developed model of the Mylar-dielectric capacitor described in Ref. 1, and some of the difficulties that have been encountered will be discussed in connection with the description of the test model.

This report is divided into three main parts. The first part deals with the electrical storage systems used in the experiments, the second part describes the instrumentation development, and the third part describes the diagnostics and results. The main and common feature of the storage systems is the pulse-charging operation. All three systems, the water-Mylar-dielectric capacitor, the water-dielectric capacitor, and the model Mylar-dielectric capacitor (designated as systems WM, W, M, respectively) have another common feature — their very low inductance, which for typical loads (exploding wires) have respective discharge frequencies of 12, 2.0, and 10 Mc/sec.

The experiments performed using these systems are divided into three categories: the measurement of the x-ray emission, the observation of light emission in the visible, and the attempts to confine the current flow in the exploding conductor. All three groups had as their common denominator the need to understand the processes occurring in the explosions of conductors when very high voltages are used. In the first group of experiments it was established that the exploding conductors emit soft x-radiation in certain circumstances. The duration of the emission was found to be quite short (about 10^{-8} sec) and related to the electrical behavior of the discharge. The emission was further analyzed and an electron temperature of a few kev associated with it. The study of the exploding conductors after the emission of x-rays ceased was performed using spectroscopic techniques in the visible range. Typical spectra are included in the report and will be seen to consist of continuum and line radiation. Both types of spectra were studied and some limits on temperature have been obtained.

The instrumentation needed for the measurement of the experimental parameters is grouped into the following categories: equipment for electrical measurements (voltage and current measuring devices and radiation measuring devices), equipment for photographic measurements (primarily, spectroscopy in the visible range and

x-ray absorption analysis), and special equipment such as explosion chambers. More emphasis is placed in the report on those instruments that have not been discussed in Ref. 1 covering the work done in the period (March 1, 1958 to June 30, 1960) preceding that which is summarized here. For this reason, streak cameras and spectrographs are not discussed. Similarly, the Laboratory facility has been adequately described in Ref. 1 and only minor changes were introduced.

ENERGY STORAGE SYSTEMS

The exploding wire experiments introduced in the preceding section were carried out using storage system WM (water-Mylar-dielectric capacitor) and storage system W (water-dielectric capacitor). These two energy storage systems have remained, except for some minor improvements, essentially as described in Ref. 1. A third system, M (model Mylar-dielectric capacitor), was built to provide a smaller, more versatile unit for studying the causes of breakdown in the large Mylar capacitor described also in Ref. 1. This model was made with the same spacing (2 feet) and geometry between the charged plate (indicated as the center plate in Fig. 1) and the grounded steel tank as that of the large Mylar capacitor. It has been designed so that the tank can be evacuated.

Tests with this model were very disappointing. The model was tested under evacuated conditions (10^{-4} mm Hg), and breakdown occurred at only 26 kilovolts. Efforts to improve conditions by replacing four layers of Mylar nearest to the high-voltage plate with polyethylene were unsuccessful. It is thus concluded that a vacuum-Mylar or vacuum-polyethylene interface has very poor breakdown characteristics.

The system M was then evacuated and filled with transformer oil which had been degassed in a large evacuated tank. Under these conditions, breakdowns occurred on various tests from 320 to 340 kilovolts. These breakdowns occurred from the point where the high-voltage cable entered the bottom Lucite cover plate. No evidence of paths by which these breakdowns reached ground could be found. In all these tests, the plate was charged to breakdown voltage in about 5×10^{-6} sec. Such approaches were concluded to be fruitless and were therefore abandoned.

The use of demineralized water in the WM system having 1-foot lengths of water-Mylar interface

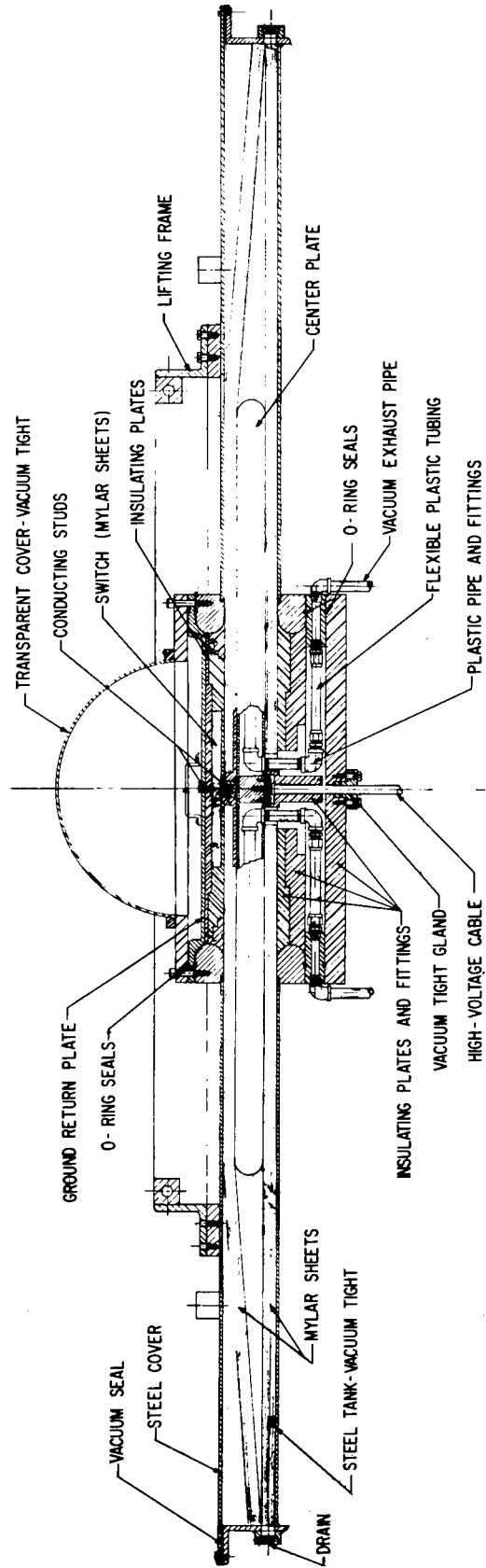


Fig. 1 - Model Mylar-dielectric capacitor. The center plate is 4 feet by 4 feet.

has been successful up to 650 kilovolts, when the charging time was 0.5×10^{-6} sec.

The W system with 4-inch spacing between the plates has operated reliably without breakdown up to 320 kilovolts. Its charging time is 1.5×10^{-6} sec.

The switching of the parallel plate capacitors of the two operational systems (W, WM) relied on the overvoting of an insulator separating the electrode of the charged plate from the ground electrode. A study of the Mylar switch is summarized in Fig. 2. The voltage strength of Mylar sheets decreases from 6500 kv/cm to 3200 kv/cm as the number of sheets is varied from one to seven. The voltage buildup time leading to the above values is about 0.5×10^{-6} sec (indicated at each measurement shown in Fig. 2).

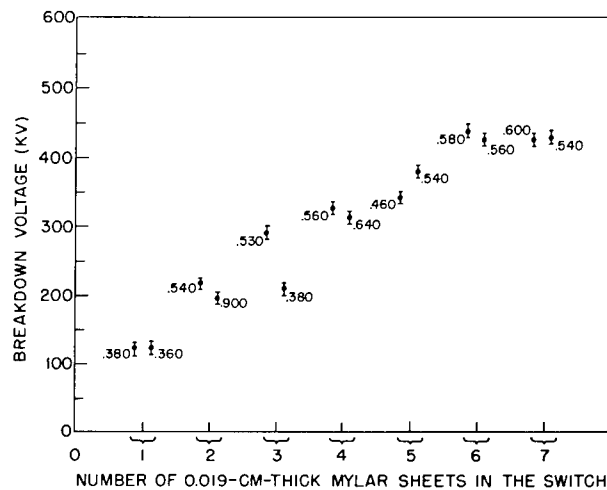


Fig. 2 - Mylar switch breakdown voltage vs switch thickness. Indicated at each measurement is the switch breakdown time in microseconds relative to the start of the applied voltage.

INSTRUMENTATION DEVELOPMENT

The instrumentation needed for the study of exploding wires developed during the period covered by this report was that for measuring the storage system circuit parameters (voltage, current, and rate of change of current) and that for study of x-ray emission from the exploding wires (pinhole camera, x-ray absorbers, and photomultiplier detectors). In addition, exploding conductor chamber development was carried out to study the electrical breakdown in the chamber parallel to the exploding conductor and means for its prevention.

A measurement with a capacitive-resistive divider provided the means for determining the instantaneous voltage on the storage capacitor plates during the pulse-charging and its subsequent discharge into an exploding conductor. The construction of the divider provides nearly perfect shielding against the magnetic pickup. Such dividers have been installed on the three storage systems. Their time response is less than 2×10^{-9} sec. The time constants of each divider were chosen to give better than 1-percent accuracies during the periods of interest. The schematic drawing of the divider and its operation is shown in Fig. 3. This divider provides the means of measuring $v(t)$ in Fig. 4.

The rate of change of current, and its time integral, the current, have been measured by the use of small well-shielded magnetic loops. Their time response is 2×10^{-9} sec. One such loop is shown in Fig. 5 in position to measure the rate of change of current in the explosion chamber. Current is obtained by integrating the $di(t)/dt$ signals with specially designed, carefully shielded RC integrating circuits.

Figure 5 is a sectional drawing of the exploding conductor chamber used in the study of the x-ray and visible radiation emitted by the exploding wires and hollow cylinders. It has eight ports for use with the diagnostic equipment, to any of which a highly shielded photomultiplier-scintillator system can be attached. The inner walls are made of nylon that serves as insulator and vacuum chamber. The difficulties encountered in using this type of explosion chamber have been extraneous discharges. It has been found that all of the discharge current flow cannot be confined to the exploding conductor when the chamber is evacuated and voltage on the plates of the capacitor is greater than 100 kv. The parallel discharge was found to go to ground points other than the ground electrode, such as the viewing ports, always choosing a path of lower inductance than that through the conductor. When these points were adequately insulated, the discharge occurred mostly through the low-pressure air surrounding the exploding conductor. Only after submerging the conductor in pure water was the discharge strongly damped. It is believed that the damping was due to all of the discharge going through the conductor.

A new explosion chamber has been built (Fig. 6) with the exploding conductor mounted horizontally instead of vertically, and with four portholes

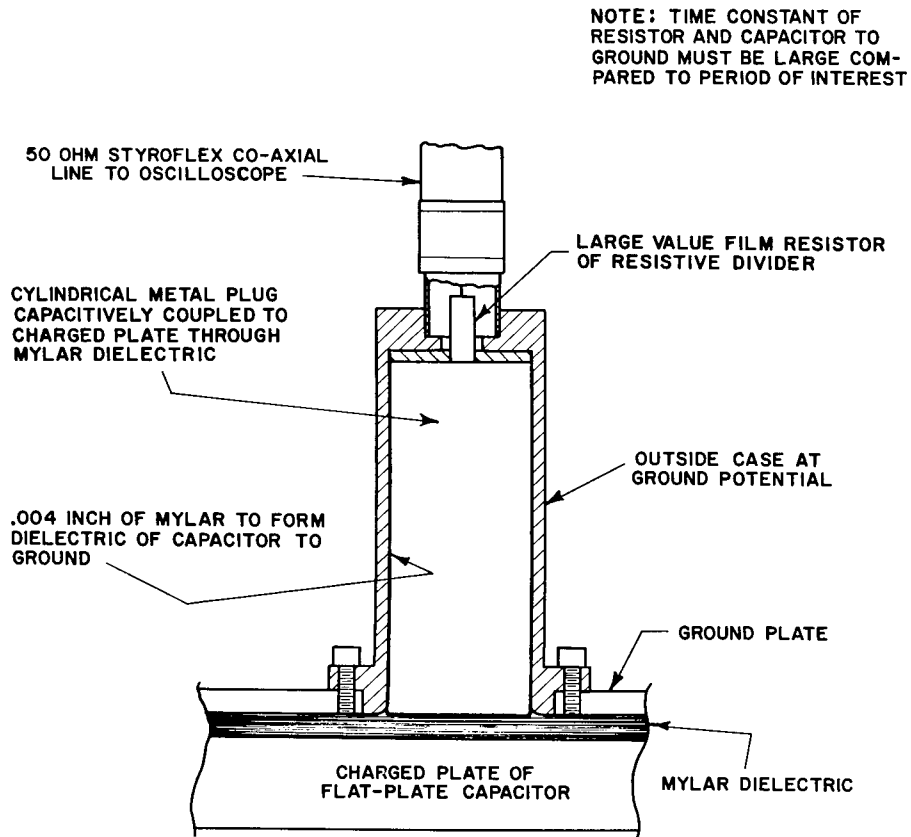


Fig. 3 - Schematic diagram of the capacitive-resistive divider to measure transient voltages on a flat-plate capacitor

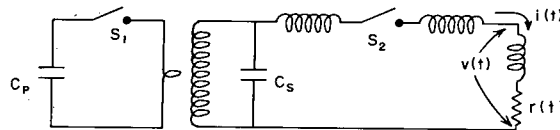


Fig. 4 - Schematic diagram of the NRL exploding-wire pulse-power systems

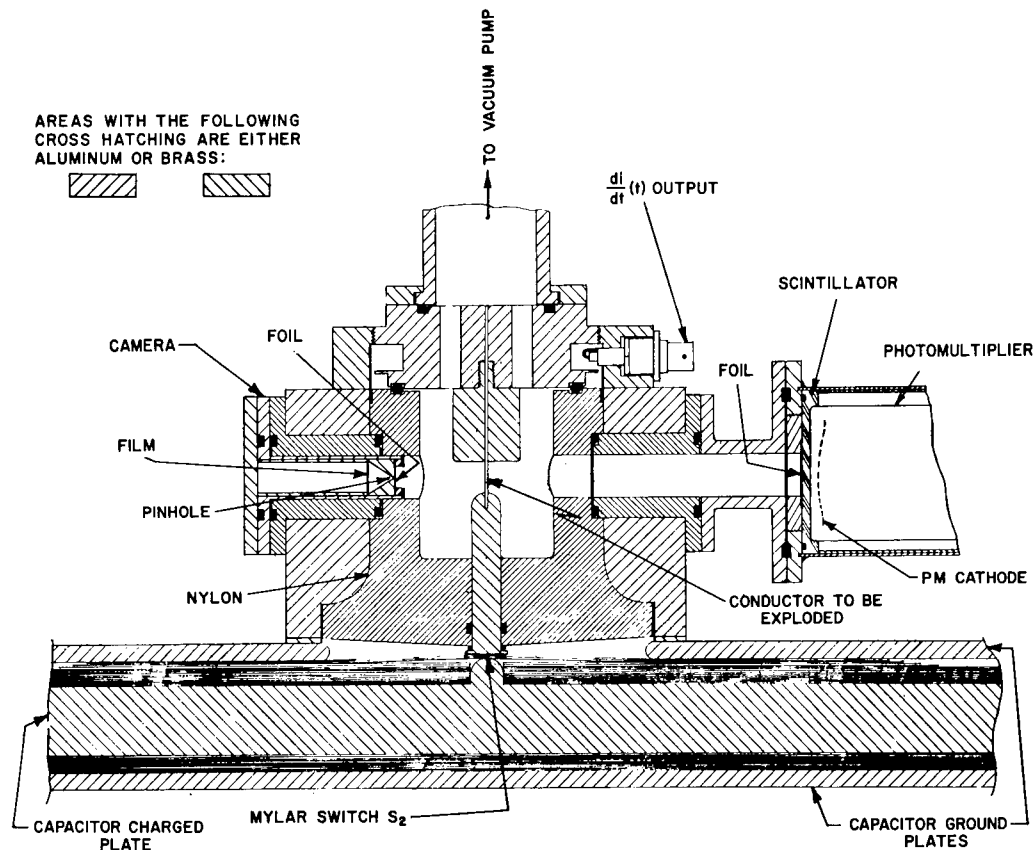


Fig. 5 - Exploding wire chamber with a magnetic loop to measure the rate of change of current $di(t)/dt$

above for diagnostic measurements. This chamber has all possible undesirable discharge paths longer than in the chamber shown in Fig. 5, and the shortest discharge path is through the exploding conductor, but the confinement of the discharge to the exploding conductor has not been achieved. Again, only submersion in pure water produced heavy damping indicating confinement of the current to the conductor.

The chamber of Fig. 6 provides the means of determining accurately the instantaneous voltage across the exploding conductor load (see the placement of the voltage divider). The voltage applied to the load in routine shots was 200 kilovolts.

When a method had been successfully devised to measure instantaneous voltage across the exploding conductor and its supporting electrodes as shown in Fig. 6, the computation of instantaneous power and resistance in the exploding conductor became more feasible. As shown by the schematic diagram of Fig. 4, power could be computed by

$$p(t) = i(t) v_r(t) = i(t) \left[v(t) - L \frac{di(t)}{dt} \right]$$

and resistance by

$$r(t) = \frac{v_r(t)}{i(t)} = \frac{v(t) - L \frac{di(t)}{dt}}{i(t)}$$

In the high-frequency (~ 12 Mc/sec), slightly damped discharges the time correlation between $v(t)$ and $L[di(t)/dt]$ must be accurate to less than 1×10^{-9} sec in order not to have large errors in the power computation. For critically damped discharges, the time correlation is not as important (2c). The time correlation can be kept accurate within 1×10^{-9} sec by applying the $v(t)$ and $L[di(t)/dt]$ signals (see Fig. 4) to opposite vertical deflection plates of an oscilloscope so that when the signal cable delays are proper and the signal

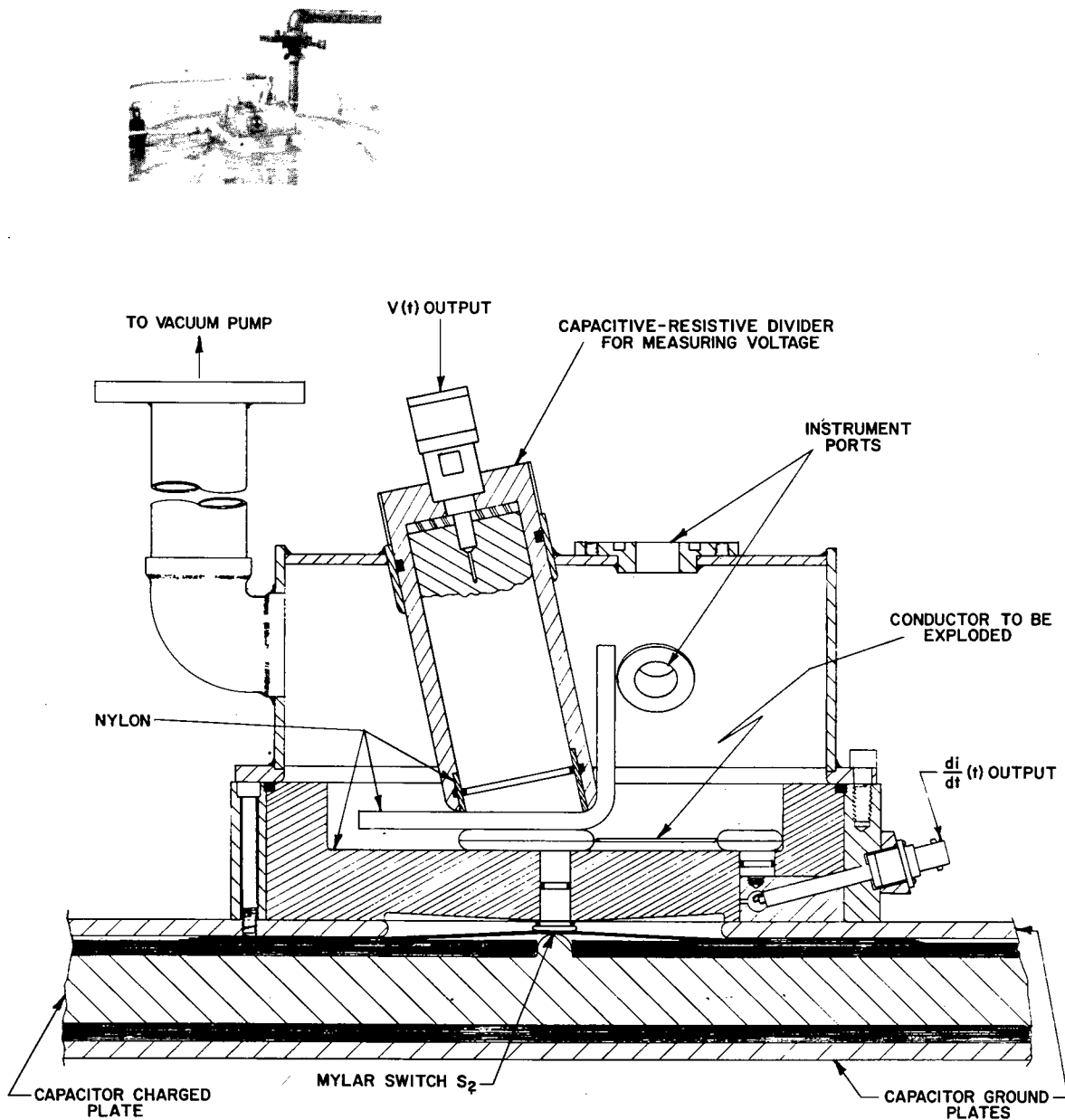


Fig. 6 - Exploding wire chamber with a voltage divider to measure the instantaneous voltage across the explosion

amplitudes are equal (for the case of zero resistance), zero deflection will result. Such an experimental example is approximated by a solid conductor which does not explode. Thus, under conditions where $r(t) > 0$ the deflection will correspond to $v(t) - L[di(t)/dt]$, which is the voltage across $r(t)$. The instantaneous current $i(t)$ is obtained by integrating the $di(t)/dt$ signal coming out of the deflection structure of the above

oscilloscope with a special RC integrator and applying it to the deflection structure of a second oscilloscope. A small-amplitude sine wave of known high frequency (compared to the frequency of the discharge circuit) can be applied to the two oscilloscopes along with a delayed $di(t)/dt$ signal in order to time-correlate the two oscilloscopes.

This approach to the power measurement assumes only that the inductance L of the exploding

wire is a constant, a condition which is true up to and during the emission of x-rays in our experiments so far. Of course, this approach requires that all of the current flows through the exploding conductor, a condition which is not met by any of these explosions in vacuum at voltages which produce x-rays. For this reason, the method has not been successful in computing power into the exploding conductors during the emission of x-rays.

In addition to the electrical instrumentation, diagnostic equipment to study the x-ray emission from the exploding conductors has been developed. A scintillator-photomultiplier-oscilloscope system with a time resolution of 9×10^{-9} sec was built and used to determine the x-ray pulse width. The mean width was found to be less than 10^{-8} sec for the majority of explosions. The scintillator used was Pilot-B plastic covered with thin Be foil such that only x-radiation could penetrate the foil. The photomultiplier used was an RCA 7265 (Ref. 4 contains time response of fast photomultipliers), while the recording oscilloscopes used were Tektronix, Model 517.

Such short x-ray pulses were also studied by means of a small pinhole camera sensitive to x-ray light only. Its position is indicated in Fig. 5. The photographs of Fig. 7 were obtained with this camera.

The quantitative study of x-rays was performed using a set of thin foils of varying thickness that partially absorb the emitted x-radiation (as discussed in the next section). The transmitted

radiation was recorded on photographic x-ray film. The relationship between the incident energy and photographic density has been obtained and is discussed in Ref. 5. The use of absorbing foils provided the only means of measuring several data points during one explosion. The more conventional means of analyzing the radiation (spectrometers and band filters) were found to have inadequate sensitivity.

The spectrographic equipment used in the study of visible and near-ultraviolet radiation is of conventional structure and is not described here. One exception is the high-dispersion, time-resolving spectrograph N9GS, which is adequately covered in Refs. 1 and 6.

EXPERIMENTAL PROCEDURE, DIAGNOSTICS, AND RESULTS

In this section the summary of the exploding conductor study is given. It is divided into two parts. The first deals with the soft x-radiation emitted during the very early stage of the explosion when the voltage across the conductor is high. The second part deals with longer lasting visible and near ultraviolet radiation characterizing the latter stages of the explosion.

The radiation emitted from the aluminum wires (0.0075 cm in diameter) in vacuum includes the soft x-radiation appearing in the first 10^{-8} sec of explosion, when the discharge is produced by the initially high capacitor voltage. The pinhole

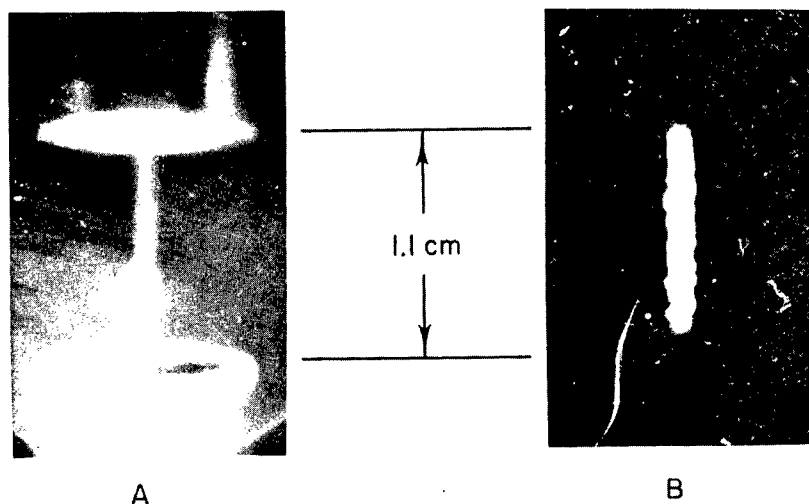


Fig. 7 - Image of a cylinder (A) by visible light before the explosion and (B) by x-rays during the explosion

cameras indicated the source of these x-rays to be the positive electrode, analogous to the pulsed x-ray tube. However, when the expansion is limited by a containing insulator (such as a plastic block), the x-radiation is then emitted from the entire length of the exploding wire. Another way of partially preventing the expansion is the use of small cylinders of the same mass as the exploding wires. The discharge through such cylinders (aluminum, 1 mm in diameter with a 0.0075-mm wall thickness) results in an implosive-explosive flow. The x-radiation under these conditions is emitted from the entire length of the wire (Fig. 7).

To study the x-radiation further, it was necessary to know the relative importance of self-absorption of the emitted x-rays in the exploding plasma. To determine this, hollow cylinders made of silver and gold were studied. No emission was noticed. However, when a small slit in a wall of such a cylinder was made, it was found that x-rays were emanating from inside the cylinders. Therefore, the self-absorption in the cylinder walls must be accounted for.

The x-rays were further studied using the absorbing foils. The radiation transmitted through thin metallic (aluminum) foils of varying thickness has been recorded by photographic film. The resulting curves of incident energy (related to the recorded density) vs the foil thickness were subjected to two methods of analysis.

First, an attempt has been made to invert the information to provide the spectrum of the emitted radiation. Only very crude information was obtained, because the absorbing foils represent a set of filters with low energy cutoff, requiring extremely precise data not available in the experiment. The simulated computer program, using the principle of x-ray fluorescence of pure elements shows that even a 5-percent error introduced randomly into 45 data points produces a rapidly oscillating inversion not resembling the trial input function. The practical number of data points (ten) gives a similar inversion. The same applied to inversion where the absorption principle is the basis of the analysis method. It thus appeared that inversion methods could not be used successfully.

The second method, developed for estimating the x-ray spectral distribution of exploding aluminum cylinders, involves a set of assumptions enumerated below and provides consistency and

error checks. The assumptions forming the basis of this method are discussed in detail below. Semi-quantitative arguments are given wherever possible to justify these assumptions.

The exploding-wire-discharge mechanism consists of acceleration of electrons by the strong applied field (~ 100 kv/cm). These electrons interact with the plasma ions. Some of the interactions are of the free-free (bremsstrahlung) and free-bound radiation transitions. It can be shown that even at electron temperatures of a few keV, the mean free paths of electrons in these transitions are on the order of 10^{-2} cm in the case of aluminum at the densities expected in the early stages of explosion (see Ref. 5; and also Ref. 1, where mean-free-path computations are given).

The length of the mean free path, relative to the entire length of the exploding conductor, justifies the assumption of the Maxwellian distribution of electron velocities. This distribution is characterized by an electron temperature T_e and the spectral distribution is given by (see Ref. 7 for units and the value of the constant C)

$$S(T_e, E) dE = C(T_e) G(E) \exp(E/kT_e) dE \quad (1)$$

where E is the radiated photon energy. Negligible self-absorption is assumed, while $G(E)$ is the Gaunt factor. If the photon energy range E is restricted such that $E > E_k$ (E_k being the K -series photon energy), and if $G(E)$ is the weighted sum of the Gaunt factors for both types of radiation, then Eq. (1) describes the photon-energy dependence of the spectrum of the bremsstrahlung and free-bound radiation. In the range E , of interest here, $G(E)$ is approximately constant and was assumed thus in further analysis (5).

In addition to bremsstrahlung and free-bound radiation, K -series lines are also present in the radiation emitted by the exploding conductors. This radiation does not contribute appreciably to the intensities measured by the absorption-foil technique discussed above. Comparison of the bremsstrahlung and ionization cross sections shows the K -series line emission to constitute about 5 percent of the total emission.

On the basis of the above assumptions, the relative intensity of the radiation emitted by the exploding conductors and subsequently partially absorbed by material of thickness x is given symbolically by

$$Y(x, T_e) = \int_0^{\infty} F(E) S(T_e, E) A(x, E) dE \quad (2)$$

where T_e is the electron temperature produced by the explosion and determines the spectral distribution $S(T_e, E)$, $F(E)$ describes the spectral response of the recording film, and $A(x, E)$ is the factor describing the absorption of photons of energy E in foils of thickness x and is taken to depend on photon energy E as $\exp[B(x)E^{-n}]$ for $E > E_k$. The values of $B(x)$ and n can be determined from tabular data of Ref. 8.

Equation (2) can be solved to obtain T_e in terms of foil thickness $x = x_1$ and $x = x_2$ by means of a saddle-point method using data for $F(E)$ in Ref. 5. The solution is

$$kT_e = \frac{1}{n} \left[\frac{(n+1)(B_2^{1/n+1} - B_1^{1/n+1})}{\frac{n+1}{2} \ln\left(\frac{B_2}{B_1}\right) + \ln\left(\frac{Y(x_1, T_e)}{Y(x_2, T_e)}\right) - \ln\left(\frac{f[E_0(x_1)]}{f[E_0(x_2)]}\right)} \right]^{\frac{n+1}{n}} \quad (3)$$

Here, $B_{1,2} = B(x_{1,2})$, and E_0 correspond to the maximum of the integrand of Eq. (2) and depend on T_e . Equation (3) is therefore an implicit equation and must be solved by iteration.

The data to be used in Eq. (3) is given in Fig. 8. A check of temperature computed from Eq. (3) has been obtained using Fig. 8. There the integral of Eq. (2) is plotted for several values of T_e and

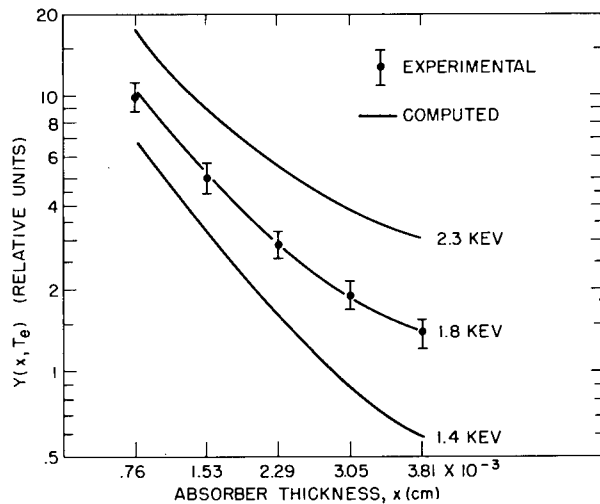


Fig. 8 - Comparison of measured x-ray outputs $Y(x, T_e)$ with curves computed from Eq. (2) for $T_e = 1.4, 1.8,$ and 2.3 keV

the best fit is used to determine T_e . Data from a typical experiment plotted in Fig. 8 is seen to correspond to a temperature of 1.8 keV. The same data used in Eq. (3) yields a temperature of 1.86 keV when a correction due to transmission of analyzing absorbers in the $E < E_k$ range is incorporated.

The analysis of the x-ray output of the imploding-exploding conductors has shown, provided the enumerated assumptions that have been made are correct, that the emitted radiation is the result of the free-free and free-bound radiation. The electron temperature, a characteristic of this type of radiation is in the low keV range and is much higher than the average ion temperature of the plasma. The errors associated with the computation of the temperature are only estimated,

but the analysis is inherently such that various errors tend to be minimized.

The analysis sketched above consists of using two parallel methods, one analytic and the other graphical. The good agreement between the two approaches suggests that it is sufficient to take only two absorption data points to compute the electron temperature. The various corrections introduced in the analytical approach seem to be appropriate, since otherwise no agreement with the graphical method would exist.

The analysis of the x-ray emission using photomultiplier tubes instead of the photographic film in order to provide a time history of the electron temperature has not been found to be feasible. This is due to the short duration of the x-ray pulse and relatively slow response of the scintillator-photomultiplier-oscilloscope system discussed in the preceding section. Figure 9 shows the responses of the system to the test impulse (A) and to the x-rays emitted by the exploding conductor (B). Trial and error calculations show that either a rectangular input pulse 8×10^{-9} sec wide or a triangular pulse 8×10^{-9} sec wide at half amplitude passing through a system with an impulse response (A) produces the resulting signal (B). This indicates that the x-ray pulse has a mean width of

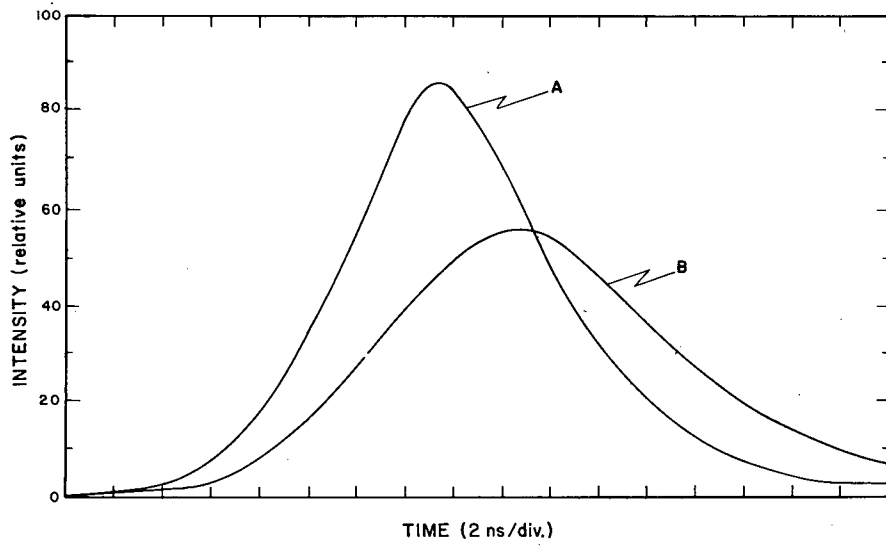


Fig. 9 - Response of the x-ray detecting system (A) to a single γ -ray input and (B) to the x-rays emitted by the explosion

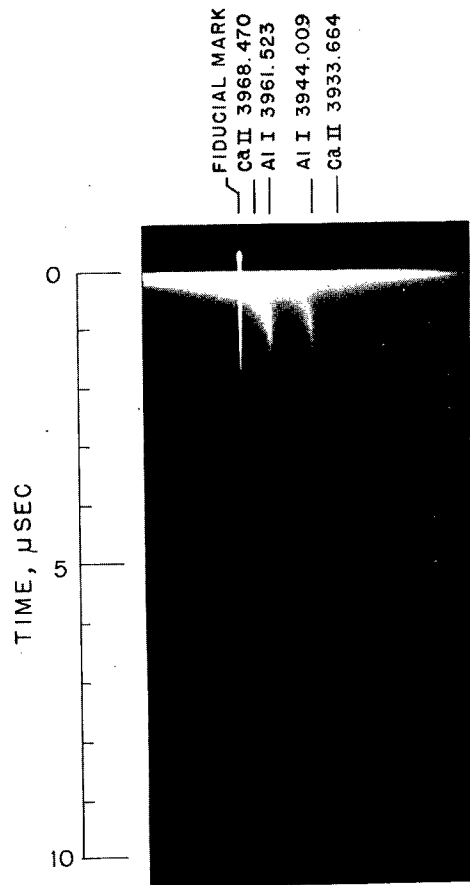


Fig. 10 - Time-resolved spectrogram of an exploding-imploding aluminum cylinder

some 8×10^{-9} sec, but its shape cannot be determined. The computation was based on the method of Ref. 9.

In addition to the x-rays emitted from the exploding wires, radiation in the visible and near ultraviolet has been studied. The study is naturally divided into the investigation of continuum emission occurring in the early stages of the explosion (first 2×10^{-7} sec after the initiation of the explosion) and the line emission which follows. This division is evident in Figs. 10 and 11 which have been obtained using the time-resolving spectrograph N9GS (described in Refs. 1 and 6). The explosions of conductors discussed have been produced using the WM system. The rise time of the emitted radiation was determined to be about 10^{-8} sec.

The investigation of the visible range has been limited by the time resolution, the dispersion and the wavelength range of the N9GS instrument. The first two limitations were imposed by the intensity of the emitted radiation. Another limitation has been the necessity to study each explosion separately. These problems are brought out in the appendix. With these limitations present, it has been possible to obtain the results given below.

The spectrogram shown in Fig. 10 (see also Fig. A1 of Appendix A) has been used to study the continuum emission. The densitometer trace

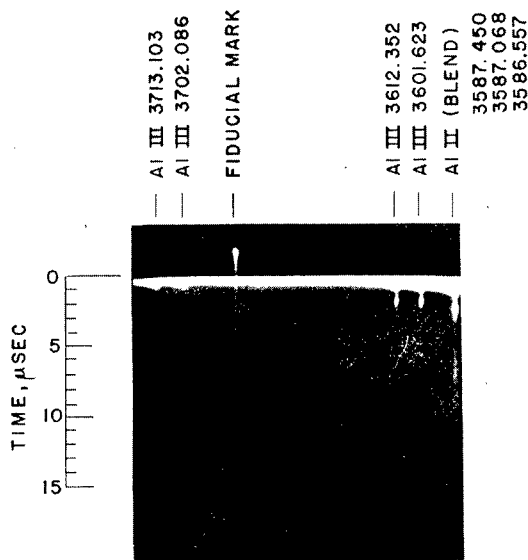


Fig. 11 - Time-resolved spectrogram of an exploding-imploding aluminum cylinder

averaged over the period 0 to 7×10^{-8} sec (one resolution-time width) was found to have only weak absorption lines superimposed on it. These were highly broadened Al I 3961.5Å and Al I 3944.0Å lines shifted some 7.5Å toward shorter wavelengths. Assuming this to be the only absorption layer present, the densitometer trace, of the initial continuum, was corrected to give the emissivity of the surface of the explosion. Estimating the emissivity accuracy to be within ± 25 percent implies a temperature of $50,000 \pm 9000^\circ\text{K}$ (equivalent to a brightness of 430 suns). The total energy emitted during the first 10^{-7} sec is therefore 1.1 joules provided no significant expansion of the exploding conductor occurs. The ratio of x-ray to visible quanta during x-ray emission is approximately 10^{-3} .

The observation of spectra of radiation emitted after extinction of the continuum emission shows that the broadening and shift of the neutral Al lines is considerable. The typical value of the shift (the Al I 3961.5Å line in Fig. 10) is 4.98Å to the red and the half-width is 16.8Å at 4.2×10^{-7} sec. The maximum expected shift of the broadened line and the broadening width due to the Doppler effect of the expanding exploding wire is 1.4Å (toward the shorter wavelengths) and 0.6Å, respectively. These values are small relative to the observed values which are caused by the electron impact and ion broadening occurring in the exploding wire plasma. Considering the instrument width to be also small, the entire shift and broadening of isolated lines (those whose width is smaller than the separation of contributing levels) is ascribed to the electron impact and ion broadening.

One such line that has been studied is that of the neutral Al (the Al I 3961.5Å line in Fig. 10) in the period from 6×10^{-7} sec until extinction. It has been found that at 6×10^{-7} sec, the temperature and the electron density of the exploding plasma are greater than $80,000^\circ\text{K}$ and 10^{18} electrons per cm^3 , respectively. At 8×10^{-7} sec, these values drop to $29,000^\circ\text{K}$ and 0.7×10^{18} electrons per cm^3 . The method used to obtain these results has been summarized in Ref. 10. The calculations have been carried out using Griem's computations of Stark broadening parameters (which are to be published in the future as an NRL Report). The computations are limited to temperatures below $80,000^\circ\text{K}$.

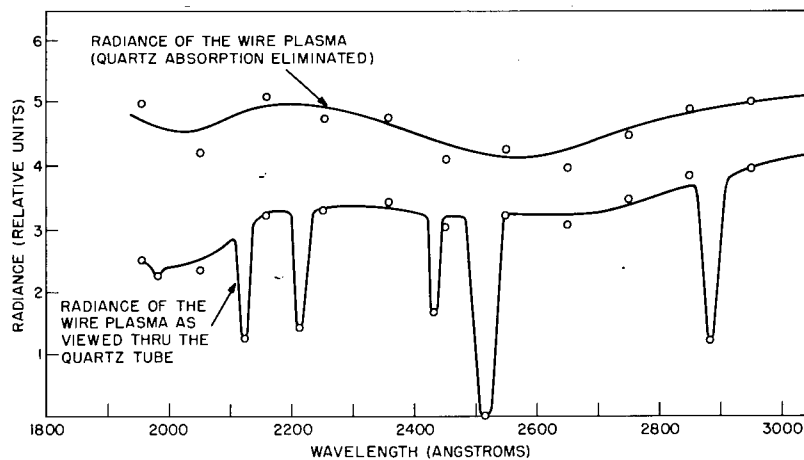


Fig. 12 - Relative radiance of an exploding aluminum wire (0.003 in. in diameter by 2-1/2 in. long; voltage on the W capacitor, 140 kv)

The electron density values obtained from the Stark broadening and shift are within 10 percent of the calculated value, since the calculation does not depend strongly on the temperature (smaller than $T^{1/6}$ dependence) and deviations from equilibrium have small effect (10; and 11, p. 189) if the isolated lines are considered.

Although the Stark broadening of the Al ion lines can be computed similarly as that for neutral lines, the computations disagree severely with the experiment. An example is provided by the Al II 3586.6Å line, for which a large shift is predicted but not observed in Fig. 11. The discrepancy is due to the effect of larger electron concentration around the attracting ion which has not been included in the structure of the theory of Ref. 10.

Computation of the Al ion line, the Al II 3586.6Å line, has shown that the measured shift is much smaller than that computed on the basis of the observed width (see Fig. 11). No computations for the Al III lines of Fig. 11 were made.

The discussion of the assumptions involved in the above approach and more detailed presentation of the data analysis of the Al I 3961.5Å line of Fig. 10 and the Al II 3586.6Å ion line of Fig. 11 is to be found in the appendix.

The plasma temperature and electron density were also determined using the Saha equations and relative intensities of two lines of a single species. A typical measurement using Al III lines indicated a 25,000°K temperature 10^{-6} sec after initiation of the explosion. If, further, the plasma is assumed to be optically thin, the average electron density at that time was found from Al II and

Al III lines to be 1.8×10^{17} electrons per cm^3 . This value is quite uncertain, since it is suspected that Al⁺ and Al⁺⁺ ion regions may not be coincident in the plasma of the exploding conductor, as an example in the appendix shows.

In addition to the spectroscopic investigation of exploding Al wires, using the WM capacitor, the W capacitor was used in the study of the near ultraviolet spectrum occurring in the explosions of Al wires in vacuum. The rise time of the emission is about 5×10^{-7} sec. Its time-integrated spectrum of a band from 1950Å to 3050Å is shown in Fig. 12. The spectrum shows Si absorption lines due to the interaction of the plasma with the quartz container of the exploding wire. The intensity of the radiation is the outstanding feature. The exploding wire output per microsecond in the 2600Å to 2800Å band was found to be about 150 times that of an Edgerton, Germeshausen, and Grier FX-100 xenon flash lamp driven by 140 μf charged to 1000 volts.

CONCLUDING REMARKS

This report is a summary of the work performed during the previous three-year period, and represents a final report to DASA on the exploding conductor research carried out by the Naval Research Laboratory.

The major accomplishments during this period are briefly as follows:

1. Techniques have been developed to observe and measure the rapidly varying currents and extremely high voltages of the discharge systems.

2. It was discovered that x-rays were produced under certain conditions by exploding conductors. The electron temperature of the plasma was deduced under the assumption that the mechanism producing the radiation was primarily free-bound radiation and bremsstrahlung. In addition, a time history of the x-ray emission was obtained which indicated that the x-rays were emitted at times of the order of 28×10^{-9} sec after initiation of the discharge and that the radiation persisted for times of the order of 8×10^{-9} sec.

3. Spectrographic studies were also made to determine the temperature and densities. Observations made in the continuum were used to deduce an "average" temperature, during the period from initiation up to 7×10^{-8} sec. After extinction of the continuum, the Stark broadening of emission lines was used to estimate the electron densities. The plasma temperature and particle densities were also determined by using the relative intensity of two adjacent lines of the same species and applying the Saha equation.

4. In addition to the temperature and density measurements mentioned above, spectrographic investigations were made of the near ultraviolet emission produced by exploding Al wires in vacuum using the W capacitor.

REFERENCES

1. Langworthy, J.B., O'Rourke, R.C., Shuler, M.P., Vitkovitsky, I.M., Dobbie, C.B., Veith, R.J., and Hansen, D.R., "Electrically Exploded Wires—Experiment and Theory, Progress Report for March 1, 1958 to June 30, 1960," NRL Report 5498, May 5, 1961
- 2a. O'Rourke, R.C., "Model Studies Quarterly Progress Report (Period Ending January 1, 1960)," progress report to the Defense Atomic Support Agency, NRL letter 7410-316:RCO'R:dh, Serial 00949/RD, Jan. 18, 1960
- 2b. Bey, P.P., Faust, W.R., Fulper, R., Jr., Leavitt, G.E., Shipman, J.D., Jr., Veith, R.J., and Vitkovitsky, I.M., "Exploding Wire Studies (Period 1 August to 1 November 1960)," progress report to DASA, NRL letter 7401-360:WRF:dh, Serial 12666, Dec. 2, 1960
- 2c. Bey, P.P., Faust, W.R., Fulper, R., Jr., Leavitt, G.E., Shipman, J.D., Jr., Veith, R.J., and Vitkovitsky, I.M., "Exploding Wire Studies (Period 1 November 1960 to 1 February 1961)," progress report to DASA, NRL letter 7440-18:GEL:ec, Serial 2207, Mar. 10, 1961
- 2d. Bey, P.P., Faust, W.R., Fulper, R., Jr., Leavitt, G.E., Shipman, J.D., Jr., Veith, R.J., and Vitkovitsky, I.M., "Exploding Wire Studies (Period 1 February to 1 May 1961)," progress report to DASA, NRL letter 7401-109:WRF:cy, Serial 5103, June 6, 1961
- 2e. Bey, P.P., Faust, W.R., Fulper, R., Jr., Leavitt, G.E., Shipman, J.D., and Vitkovitsky, I.M., "Exploding Wire Studies (Period 1 May to 1 August 1961)," progress report to DASA, NRL letter 7401-133:WRF:cy, Serial 8674, Sept. 13, 1961
- 2f. Bey, P.P., Faust, W.R., Fulper, R., Jr., Harrington, F.D., Leavitt, G.E., Shipman, J.D., Jr., and Vitkovitsky, I.M., "Exploding Wire Studies (Period 1 August to 1 November 1961)," progress report to DASA, NRL letter 7401-145:WRF:dh, Serial 11309, Dec. 8, 1961
- 2g. Bey, P.P., Faust, W.R., Fulper, R., Jr., Leavitt, G.E., Shipman, J.D., Jr., and Vitkovitsky, I.M., "Exploding Wire Studies (Period 1 November 1961 to 1 February 1962)," progress report to DASA, NRL letter 7401-13:WRF:dh, Serial 3374, Mar. 15, 1962
- 2h. Bey, P.P., Faust, W.R., Fulper, R., Jr., Leavitt, G.E., Shipman, J.D., Jr., and Vitkovitsky, I.M., "Exploding Wire Studies (Period 1 February to 1 May 1962)," progress report to DASA, NRL letter 7401-29:WRF:dh, Serial 7384, June 21, 1962
- 2i. Faust, W.R., Fulper, R., Jr., Leavitt, G.E., Shipman, J.D., Jr., and Vitkovitsky, I.M., "Exploding Wire Studies (Period 1 May to 1 August 1962)," progress report to DASA, NRL letter 7401-50:WRF:dh, Serial 12084, Oct. 23, 1962
- 2j. Faust, W.R., Leavitt, G.E., Shipman, J.D., Jr., and Vitkovitsky, I.M., "Exploding Wire Studies (Period 1 August to 1 November 1962)," progress report to DASA, NRL letter 7401-1:WRF:bjz, Serial 454, Jan. 14, 1963
- 2k. Faust, W.R., "Support Effort—Al5(h), Nuclear Weapons Effects Research Semi-Annual Progress Summary (1 July 1962 to 31 December 1962)," progress report to DASA, NRL letter 7401-19:WRF:bjz, Serial 2522, Mar. 18, 1963
3. Vitkovitsky, I.M., Bey, P.P., Faust, W.R., Fulper, R., Jr., Leavitt, G.E., and Shipman, J.D., Jr., "Exploding Wires as a Source of X-Rays," p. 87 in "Exploding Wires," Vol. II, W.G. Chase and H.K. Moore, editors, New York: Plenum, 1962
4. Lawrence Radiation Laboratory Counting Handbook, UCRL 3307 Rev. (1959)
5. Vitkovitsky, I.M., "X-Ray Emission from Exploding Conductors," University of Maryland, M.S. Thesis, 1963
6. Harrington, F.D., "An f/6.6 High-Dispersion Time-Resolving Grating Spectrograph," NRL Report 5533, Sept. 1960
7. Jahoda, F.C., Little, E.M., Quinn, W.E., Sawyer, G.A., and Stratton, T.F., Phys. Rev. 119:843 (1960)
8. Ehrenfried, C.E., and Dodds, D.E., "X-Ray Mass Attenuation Coefficients in the 1.49 to 11.9 keV Range," AFSWC-TN-59-33, Jan. 1960
9. Talbot, R.V., Shipman, J.D., Jr., Huggin, F.E., and Dobbie, C.B., NRL Report 4354, Apr. 1954
10. Griem, H.R., Phys. Rev. 128:515 (1962)
11. Griem, H.R., Baranger, M., Kolb, A.C., Oersted, G., Phys. Rev. 125:177 (1962)

Appendix A

Time-Resolved Spectroscopy in the Visible Region

One of the purposes of the spectroscopy study of the visible band was to determine the capabilities and limitations of the time-resolved spectrographic instruments (the most suitable being the N9GS spectrograph of Ref. 1) with regard to obtaining useful information from the spectra of exploding conductors. The study was applied to the *raies ultime* lines. Some of the conclusions are given below. At first, an attempt was made to analyze the spectroscopic data by treating the explosion as a blackbody source. Since the assumption of blackbody radiation at early times has not been substantiated, another approach based on the theory of Stark broadening has been carried out to permit the analysis of some strongly shifted and broadened lines.

The study of the visible spectra with the N9GS, with emphasis on time resolution and spectral line shapes leads to the following conclusions:

1. The spectrograph is capable of yielding a good time history of phenomena occurring after the electrical discharge has ceased. Continuum emission from a conductor exploded in vacuum, using the WM capacitor, persists for about 0.5×10^{-6} sec after the initiation of the explosion; it is distinct from the line structure appearing after 0.5×10^{-6} sec. Al I neutral lines last as long as 12 to 14×10^{-6} sec. Typically, the ion lines, as for instance, Al II and Al III last for about 7×10^{-6} and 2×10^{-6} sec, respectively. The Al IV lines are not in the sensitive range of the instrument. The amount of light does not constitute a problem as long as the study is confined to the strongest lines.

2. The time resolution of the N9GS is not sufficient to study in detail the emission during the time when the electrical energy is being put into the exploding conductor. This, however, is an essential requirement if the x-ray and visible spectra are to be correlated. The method of calculating the ion temperature from the observed intensities of the continuum at two different wavelengths becomes inaccurate, since the intensity does not vary sufficiently over the narrow span (140A) of the spectrograph. To measure the ion temperature in this manner it would have to be less than 10,000°K. However, an absolute measurement of the emitted radiation provides an ion

temperature averaged over the time of resolution ($\sim 0.7 \times 10^{-7}$ sec). The temperature measurement is discussed in the main text.

3. The wavelength resolution of the N9GS is sufficient to study the lines with highly pronounced wavelength shifts and broadening (for instance, Al I lines in Fig. 10). The resolution is not sufficient, however, to observe the Doppler shifts due to plasma expansion (for observed velocities of some 10^6 cm/sec).

In view of the above limitations, it was decided to analyze the spectroscopic data in order to obtain the temperature and the electron density of the plasma at late times (10^{-6} sec).^{*} The procedure and the assumptions made are as follows: First, a static, time-integrated spectrogram, obtained with a survey prismatic spectrograph showed that Al I, Al II, and Al III atomic systems were present in the near ultraviolet and visible regions during the conductor explosion. Since the N9GS time-resolved spectrograph records only a small spectral region of approximately 140A at one time, the survey spectrogram serves as a basis for selection of regions to be time resolved.

The temperature and electron density determination was attempted on the assumption that a Boltzmann distribution of ion energies exists in the plasma. If I_λ is the intensity of the emission of the plasma at wavelength λ , then

$$\frac{I_{\lambda'}}{I_{\lambda''}} = \frac{g_1 A_1 \lambda''}{g_2 A_2 \lambda'} e^{-(E_1 - E_2)/kT} \quad (A1)$$

where g_1 and g_2 are statistical weights ($2J+1$) for the upper energy levels, A_1 and A_2 are calculated spontaneous transition probabilities, E_1 and E_2 are the excitation potentials of the upper energy levels, k is the Boltzmann constant, T is the absolute temperature, and λ' and λ'' are wavelengths pertaining to the same ion species. Equation (A1) was applied to doubly ionized Al lines $\lambda' = 3612\text{A}$ and $\lambda'' = 3713\text{A}$ (shown in Fig. 11). It is essential to use the same ion species, since the distribution of

^{*}F.D. Harrington, "Time Resolution Spectroscopy," p. 162 in "Developments in Applied Spectroscopy," Vol. 2, New York:Plenum, 1963.

each ion in the plasma can be unique (for instance, the core of the exploding conductor may contain relatively more ions of higher ionization level if it is the hotter part of the plasma). The A-coefficients of the spontaneous transition probabilities were computed according to the Bates and Damgaard method.* For these two Al III lines the coefficients are

$$A_1 = 14.3 \times 10^7 \text{ sec}^{-1} \text{ for } 3^2D-4^2P^0 \text{ (3612\AA)}$$

$$A_2 = 22.0 \times 10^7 \text{ sec}^{-1} \text{ for } 4^2P^0-5^2S \text{ (3713\AA)}.$$

Using these values and Eq. (A1), the ratio $I_{\lambda'}/I_{\lambda''}$ was computed and then plotted as a function of temperature. The values of $I_{\lambda'}$ and $I_{\lambda''}$ for these two aluminum lines were read from an actual spectrogram with a densitometer, using the appropriate H and D curves for the photographic film employed. Using the experimental ratio $I_{\lambda'}/I_{\lambda''}$ thus determined, the corresponding temperature was read from the plotted curve. Typically the temperature 1 microsecond after the start of the explosion is about 25,000°K.

If, furthermore, an additional assumption that the plasma is optically thin (at the time of the measurement) is accepted, then the average electron density in the plasma can be determined. As before, relative line intensities corresponding to singly (I^+) and doubly (I^{++}) ionized atoms were obtained from the densitometer traces. The ratio of ion densities, N^{++} and N^+ , was determined from the equation

$$\frac{I^{++}}{I^+} = \frac{g^{++} U^+ \lambda^+ A^{++} N^{++}}{g^+ U^{++} \lambda^{++} A^+ N^+} e^{-(E^{++}-E^+)/kT}. \quad (\text{A2})$$

The ratio I^{++}/I^+ is obtained from the densitometer traces, and the value of T is that obtained earlier from the Al III lines. The quantities U^+ and U^{++} are the partition functions for singly and doubly ionized atoms, which in many cases, including that considered here, are approximately equal to the statistical weights g^+ and g^{++} for the ground states of the ions. The Al II and Al III lines used in the computation of the ion density ratio are $\lambda = 3586.6\text{\AA}$ and $\lambda = 3601.6\text{\AA}$, respectively. The ratio N^{++}/N^+ was found to be 34.2.

*D.R. Bates and A. Damgaard, Phil. Trans. A242:101 (1949).

Since the temperature T and the ratio of ion densities is now determined, the substitution of these values into the Saha equation yields the electron density N_e . One formulation of the Saha equation is

$$N_e \frac{N^{++}}{N^+} = \frac{2 U^{++}}{U^+} \left(\frac{2\pi m k T}{h^2} \right)^{3/2} e^{-\chi^+/kT} \quad (\text{A3})$$

where m is the electron mass and χ^+ is the ionization potential of the singly ionized system. It is obvious that for this degree of ionization (neglecting the next degree of ionization; *i.e.*, letting $N^{+++}=0$)

$$N_e = N^+ + 2N^{++}. \quad (\text{A4})$$

From Eqs. (A3) and (A4) and the known ratio N^+/N^{++} the densities of singly and doubly ionized aluminum atoms (N^+ and N^{++}) are obtained. The value of N^+ is $2.58 \times 10^{15} \text{ cm}^{-3}$ and N^{++} is $8.82 \times 10^{16} \text{ cm}^{-3}$. The value of N_e obtained for a typical explosion at $t = 10^{-6} \text{ sec}$ is $1.8 \times 10^{17} \text{ electrons/cm}^3$.

The method outlined above yields a value of N^{++}/N^+ much too high for the computed temperature (Appendix B of Ref. 1) indicating that some of the assumptions may be wrong or that there is too much variation between the two exploding conductor discharges to give a consistent value of T and N_e .

The information provided in the spectrograms, however, allows another approach to the determination of the electron density. It has been noted that Al I lines are highly shifted, some as much as 17\AA at a time soon after the continuum emission begins to weaken. This shift and the accompanying broadening is a measure of the electron density according to Stark broadening theory. The most comprehensive theory, that of Griem* is used at present to compute the electron densities from the broadening and the shift of Al I and Al II lines.

Figures 10 and A1 show very definite broadening with half-widths on the order of 10\AA and a shift toward the red of the neutral Al I 3944\AA and 3961.5\AA lines at the time of their emergence from the continuum. That the entire shift is not due to

*Reference 10 of the main text; the computation of Stark broadening parameters for various elements will be published by Griem in a future NRL Report.

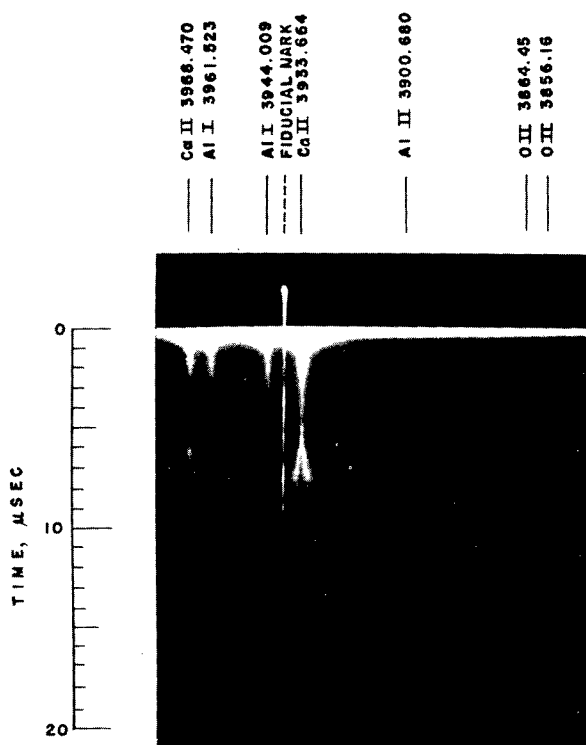


Fig. A1 - N9GS streak spectrogram of an exploding Al conductor

the Doppler effect is seen when one considers that the expanding wire material is moving toward the observer (spectrograph), thus requiring a shift toward the blue region. The alternative mechanism that can produce such shifts is the Stark effect. Now the possibility exists that the two effects are combined, and it is pertinent to see what fraction of the total shift should be ascribed to the Doppler effect. The representative velocity v of the explosion is 10^6 cm/sec. Therefore, the amount of shift $\lambda - \lambda'$ is seen to be 0.14A as given by

$$\lambda = \lambda' \left(1 + \frac{v}{c} \right) \quad (\text{A5})$$

(and $\lambda - \lambda'$ is 1.32A if v is taken to be 10^7 cm/sec). Such a magnitude of the shift is small compared to that obtained in the experiments, i.e., some 5.0A, toward the red, measured at an early time ($\sim 0.4 \times 10^{-6}$ sec) after the initiation of the explosion. The possible Doppler effect is, therefore, neglected. It is used later only in estimating the errors

involved in determining the temperature from the Stark effect.

Similarly, the broadening of neutral and ion lines is considered entirely due to the Stark effect, since again the temperature Doppler broadening given by the half-width value

$$\Delta\lambda_{1/2} \approx 2.44 \times 10^{-3} \left(\frac{T}{M} \right) \lambda \quad (\text{A6})$$

(T is the temperature in kev and M is the atomic weight of the exploding plasma) results in an increase in the half-amplitude width of only 0.6A for the case of 10^6 °K (a temperature which is higher than that attainable in the exploding conductor experiments described here). For comparison the $\Delta\lambda_{1/2}$ observed at early times is 8.0A in the case of the Al I 3961.5A line.

Having made the assumption that the Stark effect is entirely responsible for the shift and broadening of the Al I lines (3961.5A and 3944.0A), the data are now analyzed on the basis of the theory developed in a series of papers by Griem and others, for instance, Refs. 10 and 11. The most pertinent paper for the application to the Al plasma is that of Griem (Ref. 10, "Stark Broadening of Isolated Spectral Lines From Heavy Elements in a Plasma"). This paper calculates the electron impact widths w , the relative shifts d/w , and the ion broadening parameter α , using up to five interacting states for electron densities $N' = 10^{16}$ cm $^{-3}$. The results can be applied to other densities N , since w need only be multiplied by N/N' . The results given in Ref. 10 are given for cesium and argon, but the computing program set up at the National Bureau of Standards processes also aluminum and other elements and the results will be published in the future. In extending the results to higher densities, care must be taken that the ratio R of the mean ion separation distance to the Debye radius, given by

$$R = 2^{-1/6} 15^{1/3} e N^{1/6} (kT)^{-1/2} \quad (\text{A7})$$

is not more than 0.8. In the case of $N = 10^{18}$ cm $^{-3}$ and $T = 80,000^\circ\text{K}$, R is 0.33. In extending the computations to higher densities the limiting condition (Ref. 11)

$$N < N_{max} \approx \frac{mw_{\alpha'}^2}{2\pi^2 e^2} \quad (\text{A8})$$

must be observed. Here $w_{\alpha\alpha'}$ is the separation of the nearest interacting level in angular frequency units and m is the electron mass. In case of the Al I lines, $w_{\alpha\alpha'}$ is $\sim 10^{14}$ sec $^{-1}$, i.e., $N < N_{max} \approx 2 \times 10^{18}$ cm $^{-3}$.

The computation of the shift and broadening for given temperatures and electron densities is applied to the data given below as follows: the measured half-width h and the measured shift s is given (in angstroms) by the normalized formulas

$$h = 2 \times 10^{-16} N \gamma (1 + 2\alpha)$$

$$s = 10^{-16} N \gamma \frac{\beta}{\gamma} (1 + 2\alpha) \quad (\text{A9})$$

where $\alpha = (10^{-16}N)^{1/4}$, α_α , γ , and β/γ are given in Table A1. From (A9)

$$\beta/\gamma = \frac{2s}{h} \quad (\text{A10})$$

and since β/γ is a function of temperature T , then the time t can be obtained from Table A1. Table A2 lists temperature and electron density as functions of time. (The values of s that were observed are 4.98A, 2.22A, and 2.11A, and the values of h are 16.8A, 8.32A, and 4.38A for the respective times of 0.42, 0.63, and 0.84×10^{-6} sec. The instrumental broadening of 0.75A is corrected for in the above data.) If the Doppler shift and temperature broadening discussed above is assumed to affect the data above, then the resulting temperature decrease in the case of the data at 0.84×10^{-6} sec is 10 percent. At other times the effect on temperature is much smaller. Table A1 includes α_α , β/γ , and γ values for the Al II 3586.56A ion line; this line is discussed below in connection with a large discrepancy between the calculated and observed shift.

In addition to the estimate of temperature from the spectrogram of Fig. 10, the electron density N is determined. It is derived from one of Eqs. (A9) and is included in Table A2. The temperature and density values at 0.63×10^{-6} and 0.42×10^{-6} sec were obtained by extrapolating linearly the parameters of Table A1. This is not a valid procedure, since the temperature effects beyond the 80,000°K level are quite pronounced and they have not been included in the computation of values in Table A1. It is seen that

TABLE A1
Stark Broadening Parameters of Al I
and Al II Spectral Lines

T(°K)	α_α	β/γ	γ
Al I, 3961.52A			
2,500	0.0535	1.77	0.00995
5,000	0.0462	1.73	0.0121
10,000	0.0387	1.56	0.0153
20,000	0.0319	1.26	0.0198
40,000	0.0271	0.961	0.0245
80,000	0.0251	0.752	0.0271
145,000	0.0240	0.652	0.0287*
160,000	0.0237	0.574	0.0295*
Al II, 3586.56A			
2,500	0.0394	0.726	0.0136
5,000	0.0315	0.877	0.0183
10,000	0.0260	1.05	0.0237
20,000	0.0216	1.13	0.0303
40,000	0.0180	1.08	0.0387
80,000	0.0153	0.940	0.0487

*Extrapolated values.

TABLE A2
Temperature and Electron Density of the
Exploding Conductor as a Function of Time

t (10^{-6} sec)	β/γ	T (°K)	N (10^{18} cm $^{-3}$)
0.84	1.0088	29,000	0.698
0.63	0.625	145,000	1.03
0.42	0.574	>160,000	2.65

the N values are still approximately within the limit imposed by Eq. (A8).

The conclusion, therefore, is that the Stark effect can be used for estimating the temperature and computing the density in exploding conductor plasmas only after an adequately long time after the initiation of the explosion has elapsed and the plasma has become sufficiently cooled. This time is seen to be about 10^{-6} sec in the experiments discussed here, which were performed using the WM capacitor.

Table A1 also shows that the Al II 3586A ion line, because of the magnitude of the broadening, should be shifted on the order of 10Å at 25,000°K — the temperature, expected on the basis of Table A1, at 10^{-6} sec after the start of the explosion. This shift, however, is not observed (e.g., Fig. 11). The reason that the Al II 3586A ion line is not shifted is that the free electrons in the plasma tend to cluster around the Al^+ ion due to its electrostatic attraction. This results, for the densities considered here, in a shift that is estimated to be of the same magnitude but is in the opposite sense to that computed. The computations used here (Table A1) do not provide for such a clustering effect.

One additional comment should be made regarding the application of the Stark broadening

and shift to the temperature and electron density determination of exploding conductor plasmas. The dependence of the widths, in the range of applicability, calculated in Ref. 10 is very weakly dependent on the temperature (less than $T^{1/6}$ dependence) and therefore the densities can be determined even when the temperatures are not known precisely and even when one is not sure of the existence of local equilibrium (Ref. 11, p. 189). On the other hand, the line widths are somewhat distorted if the plasma observed is not completely optically transparent. This is so, since the line intensity maxima in such a case are over-emphasized because of the greater self-absorption in the line wings. Since no information regarding the transparency is available, no estimate of this effect can be made.